Charge transfer kinetics in CdSe quantum dot sensitized solar cells†

Eugenia Martínez-Ferrero,[a] Ivan Mora Seró,*[b] Josep Albero,[a] Sixto Giménez,[b] Juan Bisquert[b] and Emilio Palomares*[a]

Received 27th November 2009, Accepted 4th February 2010
First published as an Advance Article on the web 19th February 2010
DOI: 10.1039/b924970b

We report the charge transfer dynamics for CdSe quantum dot (QD) sensitized solar cells. The effect of QD sensitization mode in recombination kinetics has been measured and their implications in solar cell performance analyzed.

Dye-sensitized solar cells (DSC) based on ruthenium polypyridil complexes have dominated the topic of molecular photovoltaics since the pioneer communication of O'Regan and Graetzel in the nineties.[1] In fact, recent milestones such as efficiencies as high as 11% under standard solar irradiation (100 mW cm^{-2}, 1.5 AM G solar spectrum) and 1000 h of stability under continuous light soaking have been reported.[2] Nevertheless, in parallel, a growing interest on the use of other alternatives to the ruthenium complexes did also occur with recent achievements leading to highly efficient DSC based on organic dyes containing polythiophene units.[3]

However, less attention has been paid to the use of inorganic materials, like quantum dots (QD), as sensitizers. QDs have several properties that make them suitable as good candidates for mesoporous TiO_2 sensitization like high molar extinction coefficient, chemical stability under continuous irradiation and the fact that the absorption band-gap can be tuned controlling the nanocrystal size.[4–6] Yet, only a few reports can be found in the literature addressing the interfacial charge transfer reactions occurring between the electrons at the TiO_2 nanoparticles and either the oxidised quantum dot or the oxidised electrolyte[7–9] and mainly in the case of colloidal QDs linked to TiO_2 using bifunctional linker molecules.[10] The understanding and control of these mentioned reactions is key to increase the overall device efficiency.

Herein we describe the charge transfer kinetics for DSC based on CdSe QDs coated with ZnS under illumination. Two different sensitization modes have been investigated. In both cases the QDs are directly anchored to the TiO_2 nanoparticles with the absence of linkers. The main difference between both modes results from the methodology employed to sensitize the mesoporous TiO_2 film. In one case, the QDs were synthesized as colloids and adsorbed later on the TiO_2 nanoparticle surface without any particular linker[11,12] (see ESI†). These samples are referred to from now on as **s-DAD** (direct adsorption deposition). On the other hand, the TiO_2 sensitization was also carried out using chemical bath deposition techniques and the samples are referred to as **s-CBD**.

Fig. 1 shows the photocurrent *vs.* voltage curves. Both devices show similar fill factor (FF) and open circuit voltage (V_{oc}) values (see Table 1); however, the generated photocurrent is higher in the **s-CBD** sample. This fact prompted us to undertake photophysical studies on the systems.

In both cases we obtained the desired material consisting of CdSe nanocrystals anchored onto the TiO_2 mesoporous substrate and coated with a ZnS layer. The inset in Fig. 1 shows the UV-visible spectra of the mesoporous TiO_2 sensitized film as Kubelka–Munk units. As it can be seen, we observe an excitonic peak at 567 nm which corresponds to CdSe/ZnS with a band gap of 2.18 eV. From the UV-visible we can infer that the **s-CBD** samples present much higher absorbances than the **s-DAD** films, pointing to the superior ability of the CBD technique to introduce the QD on the mesopores of the inorganic film. The steady-state fluorescence emission spectra for both sensitized films (Fig. S1†) shows a clear emission band with a single maximum centered at 585 nm for the **s-DAD** film while in the case of **s-CBD** a broad emission region is observed. The presence of a broad photoluminescence (PL) emission has been previously assigned to the presence of QDs with different size. Thus, at first glance, we can confirm that the **s-DAD** route allows a higher degree of control over the synthesis of nanocrystals although the surface coverage onto the mesoporous TiO_2 films is higher for the **s-CBD** route.

Electron injection kinetics from the QD conduction band (CB) into the TiO_2 CB can be studied using time correlated single photon counting (TCSPC). This technique has been widely used previously to assess the same charge transfer reaction in ruthenium polypyridyl dye-sensitized mesoporous TiO_2 films and complete devices.[13,14] The electron dynamics for the **s-CBD** films give results too fast for our system (see Fig. S2†), which has an instrument response (IRF) of 300 ps. Hence, we are unable to directly estimate if the lack of emission decay is due to either ultrafast electron injection or fast deactivation of the excited state before electron injection or both. Nonetheless, as shown in Fig. 1, the presence of high photocurrents (mA) for the **s-CBD** device implies that electron injection yield is efficient to some extent. In contrast, for the **s-DAD** samples the emission lifetime was measured and the experimental data was fitted to a biexponential equation (eqn (1)) with lifetimes (τ) of τ_1 = 9.1 ns (64.9%) and τ_2 = 2.4 ns (35.1%). This multiexponential decay behavior, which generates different lifetime values, has been previously

[a] *Institute of Chemical Research of Catalonia, Avda. Països Catalans, 16, Tarragona E-43007, Spain. E-mail: epalomares@iciq.es; Fax: +34 977 920 224; Tel: +34 977 920 241*
[b] *Photovoltaic and Optoelectronic Devices Group, Department de Física. Universitat Jaume I, E-12071, Spain. E-mail: sero@fca.uji.es*

† Electronic supplementary information (ESI) available: Experimental preparation of CdSe quantum dots, ZnS coating and the solar cells, description of the measurements, emission photoluminescence spectrum and emission decays. See DOI: 10.1039/b924970b

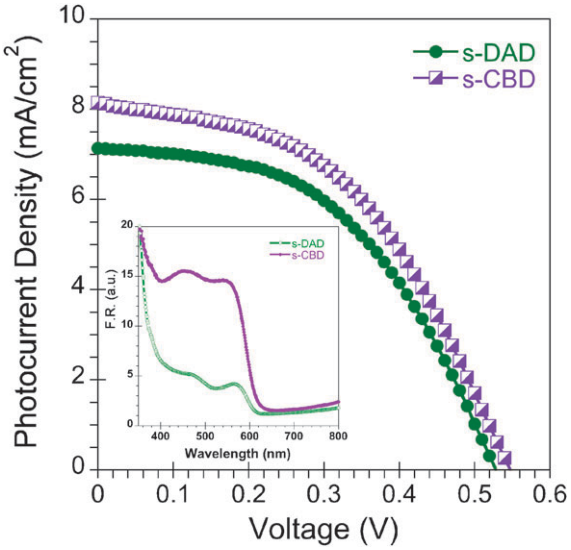

Fig. 1 *I–V* curves for the CdSe-ZnS samples studied in this work using polysulfide as the electrolyte. The cell area was 0.24 cm^2 and the light intensity was 100 mW cm^{-2}. The inset shows the UV-visible spectra of the mesoporous TiO_2 sensitized film as Kubelka–Munk units.

Table 1 Photoelectrochemical parameters obtained from the *I–V* curve of the 0.24 cm^2 devices using polysulfide as electrolyte under 1 sun illumination

Devices	J_{sc}[a]/mA cm^{-2}	V_{oc}[b]/V	FF[c]	η[d] (%)
s-DAD	7.13	0.53	0.49	1.83
s-CBD	8.15	0.55	0.47	2.01

[a] J_{sc}: current density at short circuit. [b] V_{oc}: potential at open circuit. [c] FF: fill factor. [d] η: efficiency.

observed and corresponds to the varying degree of surface defects/energy traps on the TiO_2.

$$I(t) = I_1\exp(-t/\tau_1) + I_2\exp(-t/\tau_2) \quad (1)$$

where $I(t)$ represents the time (t) dependent decay of the fluorescence intensity, I_x (x = 1, 2) stands for the initial intensity values and t_x (x = 1, 2) is the lifetime value obtained from the decay, indicating the average time that the dye spends in the excited state before returning to the ground state. The presence of two terms in the equation reflects the variety of surface states and energy traps on the TiO_2 nanoparticles.

This result indicates that the electron injection on the **s-DAD** samples is limited due to the competition between the electron injection process and the relaxation of the electrons from the excited state to the ground state.

Following our study on the interfacial charge transfer dynamics, we turn now into the recombination dynamics regarding the back electron reaction from the TiO_2 to the oxidized QD. As depicted in Fig. 2a, the transient absorption spectra (observed 100 μs after excitation of the CdSe/ZnS) exhibit a positive signal with a maximum 620–720 nm indicating charge separation at the interface. Both spectra are similar, despite the broad size distribution of the **s-CBD** sample. The transient decay dynamics of both samples (Fig. 2b) show different kinetics, which expands from a sub-microsecond to

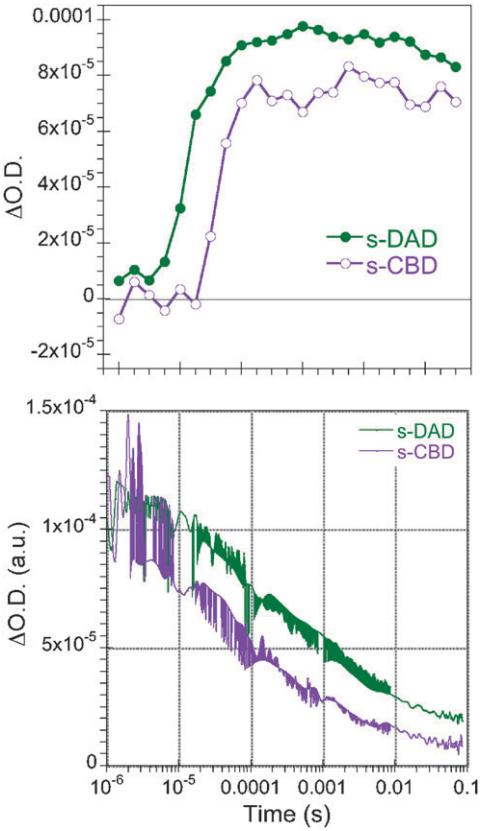

Fig. 2 (top) Transient absorption spectra recorded at 100 μs after excitation at 440 nm; (bottom) electron recombination decays of CdSe/TiO_2 after excitation at λ_{ex} = 440 nm and monitoring at λ_m = 620 nm. Analyzed electrodes on air.

a millisecond time scale with lifetimes, τ, of 0.08 ms and 1.4 ms for **s-CBD** and **s-DAD**, respectively. It has to be noted that the decays monitored at different wavelengths, corresponding to the broad maxima of the transient absorption spectra, give the same results. These stretched exponential decays ($\Delta O.D.(t) = A_0 \exp(-(t/\tau)^{\beta})$) are typical of DSC due to the trapping/de-trapping process of the photo-injected electrons while being transported through the nanocrystalline TiO_2 particles. Moreover, the decay signals do not reach a plateau at the fastest time scales (10^{-6}–10^{-5} s), which implies that the recombination processes starts at early times, after only hundreds of nanoseconds. Indeed, when comparing the electron recombination kinetics between the **s-CBD** and the **s-DAD** sensitized TiO_2 films and the TiO_2 films sensitized with the classic ruthenium polypyridyl complex **N719** (chemical name: *cis*-diisothiocyanato-bis(2,2-bipyridyl-4,4-dicarboxylato) ruthenium(II) bis-(tetrabutylammonium)) the recombination dynamics are 10 times faster in the **s-CBD** case while in the **s-DAD** has a similar back-electron transfer lifetime.[13,15] This observation can be explained if we take into account that the "*in situ*" synthesis of CdSe QDs coated with ZnS by CBD technique makes a continuous material in contact with the TiO_2 nanoparticles wetting entirely the semiconductor mesoporous surface. Thus, the distance between the oxidised **s-CBD** material and the TiO_2 surface is much shorter than the TiO_2–**N719** distance. Furthermore, we have measured the recombination dynamics in the presence of the polysulfide

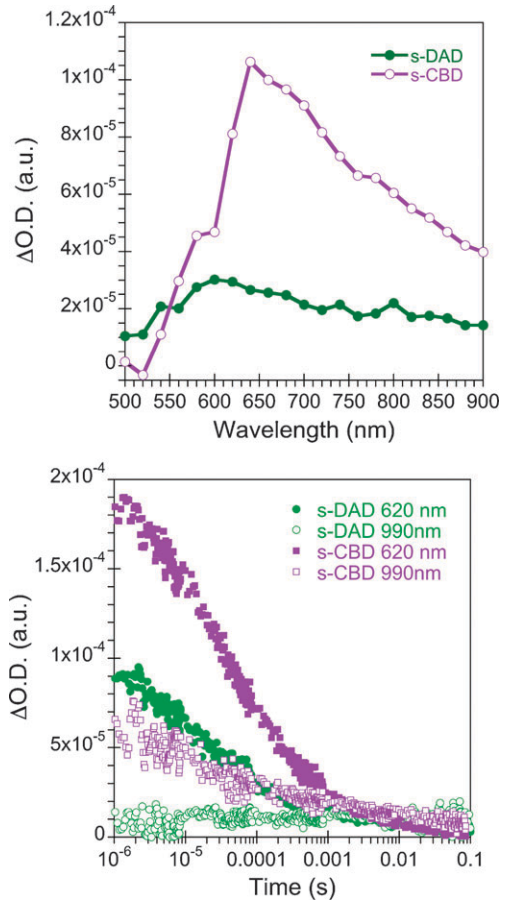

Fig. 3 (top) Transient Absorption spectra recorded at 100 μs after excitation at 440 nm; (bottom) electron recombination decays after excitation at λ_{ex} = 440 nm and monitoring at λ_m = 620 nm or λ_m = 990 nm. Polysulfide electrolyte was in contact with the analyzed electrodes.

electrolyte (Fig. 3). The transient absorption spectra, recorded after dye excitation at 440 nm, shows a positive signal in the same wavelength range than that measured without electrolyte. This signal is due to the absorption of the dye cation, and in less extent, to the absorption of Ti^{3+} species arising after electron injection from the dye. Thus, we have monitored the decay at the same wavelength than the previous spectra, 620 nm, resulting in biexponential signals. The first decay is assigned to the $CdSe/TiO_2$ recombination processes; it occurs at shorter times that the corresponding decay without electrolyte due to the effective regeneration of the oxidized QD by the polysulfide electrolyte. The second decay occurs at longer times and can be assigned to the injected electrons in the CB of TiO_2 plus the absorption signal of the $CdSe/ZnS^+$. The measurement at 990 nm allows the detection of long-lived species assigned previously by Montanari *et al.*[16] to photoinjected electrons, confirming the previous observation.

In light of these results we can foresee that the limitation on the use of the direct adsorption method will concern the efficient luminescence deactivation pathway that is limiting the efficient electron injection reaction. Nonetheless, the photocurrent achieved with the **s-DAD** samples, despite being smaller than the **s-CBD** based devices, is significant. Taking into account that the number of adsorbed quantum dots for the **s-DAD** samples is much lower than for **s-CBD**, we can infer that increasing either the amount of CdSe QDs anchored by direct adsorption, the electron injection yield, or both, will boost the device efficiency due to higher photocurrents.

In conclusion, the recombination kinetics of **s-DAD** is of the same order as the recombination for **N719** sensitized TiO_2 electrodes. Faster recombination kinetics is observed for **s-CBD** QDs. Therefore, there is a need to look for the modification of the direct adsorption method that has hitherto been used to achieve the sensitization of the mesoporous TiO_2 in order to enhance the photo-induced electron injection reaction very efficiently as well as increase the quantum dots adsorption. On the other hand, the recombination kinetics for **s-CBD** QDs has to be reduced in order to increase cell performance efficiency. In addition it has been demonstrated that polysulfide electrolyte acts as an effective regenerative electrolyte.

Acknowledgements

Dr Martínez-Ferrero, Mr Albero and Dr Giménez want to thank the MICINN for the Juan de la Cierva, Torres Quevedo and Ramón y Cajal fellowships, respectively. Prof. Palomares and Prof. Bisquert thank the MICINN for the CONSOLIDER CDS-0007 HOPE-2007 project and the projects CTQ2007-60746/BQU. Prof. Palomares also thanks the European Research Council for the ERC fellowship PolyDot. The ICIQ and ICREA support is also gratefully acknowledged. The authors want to acknowledge Dr Roberto Gómez for providing colloidal QDs.

Notes and references

1 B. O'Regan and M. Graetzel, *Nature*, 1991, **353**, 737–740.
2 F. Gao, Y. Wang, D. Shi, J. Zhang, M. Wang, X. Jing, R. Humphry-Baker, P. Wang, S. M. Zakeeruddin and M. Gratzel, *J. Am. Chem. Soc.*, 2008, **130**, 10720–10728.
3 M. Wang, M. Xu, D. Shi, R. Li, F. Gao, G. Zhang, Z. Yi, R. Humphry-Baker, P. Wang, S. M. Zakeeruddin and M. Gratzel, *Adv. Mater.*, 2008, **20**, 4460–4463.
4 P. V. Kamat, *J. Phys. Chem. C*, 2008, **112**, 18737–18753.
5 A. P. Alivisatos, *Science*, 1996, **271**, 933–937.
6 W. Yu, L. H. Qu, W. Z. Guo and X. G. Peng, *Chem. Mater.*, 2003, **15**, 2854–2860.
7 I. Robel, M. Kuno and P. V. Kamat, *J. Am. Chem. Soc.*, 2007, **129**, 4136–4137.
8 H. Lee, H. C. Leventis, S.-J. Moon, P. Chen, S. Ito, S. A. Haque, T. Torres, F. Nesch, T. Geiger, S. M. Zakeeruddin, M. Gratzel and M. K. Nazeeruddin, *Adv. Funct. Mater.*, 2009, **19**, 2735–2742.
9 Y. Tachibana, K. Umekita, Y. Otsuka and S. Kuwabata, *J. Phys. Chem. C*, 2009, **113**, 6852–6858.
10 R. S. Dibbell and D. F. Watson, *J. Phys. Chem. C*, 2009, **113**, 3139–3149.
11 S. Giménez, I. Mora-Seró, L. Macor, N. Guijarro, T. Lana-Villarreal, R. Gómez, L. J. Diguna, Q. Shen, T. Toyoda and J. Bisquert, *Nanotechnology*, 2009, **20**, 295204.
12 N. Guijarro, T. Lana-Villarreal, I. Mora-Seró, J. Bisquert and R. Gómez, *J. Phys. Chem. C*, 2009, **113**, 4208–4214.
13 A. Reynal, A. Forneli, E. Martinez-Ferrero, A. Sanchez-Diaz, A. Vidal-Ferran, B. C. O'Regan and E. Palomares, *J. Am. Chem. Soc.*, 2008, **130**, 13558–13567.
14 J. H. Bang and P. V. Kamat, *ACS Nano*, 2009, **3**, 1467–1476.
15 G. Boschloo and A. Hagfeldt, *Inorg. Chim. Acta*, 2008, **361**, 729–734.
16 I. Montanari, J. Nelson and J. R. Durrant, *J. Phys. Chem. B*, 2002, **106**, 12203–12210.